Source decomposition of eddy-covariance CO_2 flux measurements for evaluating a high-resolution urban CO_2 emissions inventory

Kai Wu[1]‡, Kenneth J. Davis[1,2], Natasha L. Miles[1], Scott J. Richardson[1], Thomas Lauvaux[3], Daniel P. Sarmiento[4], Nikolay V. Balashov[4], Klaus Keller[5,2], Jocelyn Turnbull[6,7], Kevin R. Gurney[8,9], Jianming Liang[9], Geoffrey Roest[8]

[1] Department of Meteorology and Atmospheric Science, The Pennsylvania State University, University Park, Pennsylvania 16802, United States
[2] Earth and Environmental Systems Institute, The Pennsylvania State University, University Park, Pennsylvania 16802, United States
[3] Laboratoire des Sciences du Climat et de l'Environnement, IPSL, CEA Saclay, 91191 Gif sur Yvette, Cedex, France
[4] NASA Goddard Space Flight Center, Greenbelt, Maryland 20771, United States
[5] Department of Geosciences, The Pennsylvania State University, University Park, Pennsylvania 16802, United States
[6] Rafter Radiocarbon Laboratory, GNS Science, Lower Hutt 5040, New Zealand
[7] CIRES, University of Colorado at Boulder, Boulder, Colorado 80309, United States
[8] School of Informatics, Computing and Cyber Systems, Northern Arizona University, Flagstaff, Arizona 85287, United States
[9] School of Life Sciences, Arizona State University, Tempe, Arizona 85281, United States

E-mail: kwu2@ed.ac.uk

Abstract.

We present the comparison of source-partitioned CO_2 flux measurements with a high-resolution urban CO_2 emissions inventory (Hestia). Tower-based measurements of CO and ^{14}C are used to partition net CO_2 flux measurements into fossil and biogenic components. A flux footprint model is used to quantify spatial variation in flux measurements. We compare the daily cycle and spatial structure of Hestia and eddy-covariance derived fossil fuel CO_2 emissions on a seasonal basis. Hestia inventory emissions exceed the eddy-covariance measured emissions by 0.36 μmol m^{-2} s^{-1} (3.2%) in the cold season and 0.62 μmol m^{-2} s^{-1} (9.1%) in the warm season. The daily cycle of fluxes in both products matches closely, with correlations in the hourly mean fluxes of 0.86 (cold season) and 0.93 (warm season). The spatially averaged fluxes also agree in each season and a persistent spatial pattern in the differences during both seasons that may suggest a bias related to residential heating emissions. In addition, in the cold season, the magnitudes of average daytime biological uptake and nighttime respiration at this flux site are approximately 15% and 27% of the mean fossil fuel CO_2 emissions over the same time period, contradicting common assumptions of no significant biological CO_2 exchange in northern cities during winter. This work

‡ Now at: School of GeoSciences, The University of Edinburgh, Edinburgh, United Kingdom

demonstrates the effectiveness of using trace gas ratios to adapt eddy-covariance flux measurements in urban environments for disaggregating anthropogenic CO_2 emissions and urban ecosystem fluxes at high spatial and temporal resolution.

Keywords: eddy-covariance flux measurements, source partitioning, emissions inventory, fossil fuel CO_2 emissions, biogenic CO_2 fluxes

1. Introduction

Cities are becoming the focus for formulating and implementing carbon dioxide (CO_2) emissions mitigation efforts (Hutyra et al., 2014; Lee and Koski, 2014; Bulkeley, 2013). Evaluating the effectiveness of emissions reduction efforts requires accurate CO_2 emissions estimates (Lauvaux et al., 2020; Turnbull et al., 2018). Although cities cover only 3% of the global land area, urban areas are home to 55% of the world's population, a proportion that is expected to increase to 68% by 2050 (Chaouad and Verzeroli, 2018). Overall, more than 70% of global fossil fuel CO_2 (CO_2ff) emissions are from urban areas (Edenhofer et al., 2015). Efforts to assess and mitigate CO_2 emissions can provide benefits for urban sustainability and balanced economic growth (Hsu et al., 2019).

Urban areas are consistently reported as a net source of CO_2 emissions (Velasco and Roth, 2010). The eddy-covariance technique has been applied to measure urban CO_2 emissions in different cities for about two decades (Björkegren and Grimmond, 2018; Park and Schade, 2016; Ao et al., 2016; Helfter et al., 2016; Lietzke et al., 2015; Christen, 2014; Järvi et al., 2012; Christen et al., 2011; Vogt et al., 2006; Nemitz et al., 2002; Grimmond et al., 2002). The attribution of urban CO_2 flux measurements is challenging due to the spatial heterogeneity, mixed emission sources and sinks, and limited spatial coverage of flux measurements (Aubinet et al., 2012). Although most previous studies focus on the observed net CO_2 flux, a few studies attempt to partition flux measurements into fossil and biogenic components accounting for the temporal and spatial variability of the multiple sources and sinks. Menzer and McFadden (2017) modeled fossil CO_2 emissions based on winter data and extrapolated them to the growing season to estimate biogenic fluxes. Ishidoya et al. (2020) demonstrated partitioning of CO_2 fluxes into liquid and gaseous fossil components using O_2 and CO_2 measurements. Sugawara et al. (2021) used a nearby tower to estimate the biogenic component of a total CO_2 flux measurement.

Quantification of anthropogenic CO_2 emissions is challenging due to the difficulty of separating CO_2ff emissions from biogenic CO_2 (CO_2bio) fluxes (Miller et al., 2020; Basu et al., 2020). Previous studies demonstrated the feasibility of using ^{14}C isotope measurements to separate CO_2ff from CO_2bio fluxes (Basu et al., 2016; Turnbull et al., 2015; Miller et al., 2012), but flask measurements of ^{14}C are expensive and discontinuous. Continuous measurements of carbon monoxide (CO) provide another approach to track CO_2ff emissions (Park and Schade, 2016; Silva et al., 2013; Turnbull et al., 2011; Vogel et al., 2010; Levin and Karstens, 2007). Uncertainties in the CO to CO_2ff ratio, which vary as a function of emission sectors, complicate the attribution of urban CO_2 fluxes. The use of ^{14}C measurements to determine the ratio of CO to CO_2ff has not yet been applied to eddy covariance flux measurements. We attempt to combine the complementary strengths of CO and ^{14}C to decompose net CO_2 flux measurements, and use the partitioned CO_2ff emissions to evaluate a high-resolution emissions inventory.

Emissions inventories use activity data to aggregate urban CO_2ff emissions (Olivier and Janssens-Maenhout, 2012; Boden et al., 2009; Gurney et al., 2009), but the differences among inventories are sizeable (Gurney et al., 2020; Oda et al., 2019; Gately and Hutyra, 2017). Atmospheric inversions use inventories as prior estimates of emissions and optimize the emissions using atmospheric CO_2 mole fraction observations (Lauvaux et al., 2020; Kunik et al., 2019; Lauvaux et al., 2016; Staufer et al., 2016; Turner et al., 2016; Bréon et al., 2015). Two substantial sources of uncertainty in inverse estimates of urban CO_2ff emissions are uncertain CO_2bio fluxes and unknown error characteristics in emissions inventories (Wu et al., 2018). The Hestia emissions inventory (Gurney et al., 2012) was developed in part to support the Indianapolis Flux Experiment (INFLUX) and uses energy consumption, population density, and traffic data to quantify CO_2ff emissions for an entire urban landscape at an approximately 200 m and hourly resolution. While excellent agreement between Hestia and atmospheric inversions has been shown over multiple years at the scale of an entire city (Lauvaux et al., 2020), the high-resolution performance of the Hestia inventory has not yet been evaluated with eddy-covariance flux measurements.

This study compares source-partitioned CO_2 eddy-covariance flux measurements with a high-resolution emissions inventory (Hestia) in a suburban region of Indianapolis, Indiana, USA. We partition the net CO_2 flux measurements into CO_2ff and CO_2bio components using a flux-gradient relationship (Stull, 2012) and atmospheric CO measurements. ^{14}C isotope measurements are used to estimate the CO to CO_2ff ratio and reduce the uncertainty in the flux decomposition. The source decomposition methods are similar to those used by Ishidoya et al. (2020) and Sugawara et al. (2021). In addition, we use a flux footprint model (Kljun et al., 2015, 2004) to match each flux measurement in space and time with the Hestia inventory to provide a direct comparison of independent estimates of anthropogenic CO_2 emissions at high spatial and temporal resolution. This is, to our knowledge, the first such comparison of these innovative and independent assessments of high-resolution urban CO_2 emissions, and is timely given the growing interest in monitoring the impact of urban systems on atmospheric composition.

2. Data and Methods

2.1. Site Descriptions and Atmospheric CO_2 Flux Measurements

The INFLUX observation network (Davis et al., 2017) measures atmospheric CO_2 and CO mole fractions, and net CO_2 fluxes in and around Indianapolis, IN (Figure 1). The locations, sampling heights and measurements at these sites are described by Miles et al. (2017) and the instrument performance is described by Richardson et al. (2017). ^{14}C isotope measurements, collected weekly, are used to evaluate CO to CO_2ff ratios using methods described by Turnbull et al. (2015).

Since the flux decomposition requires atmospheric measurements of CO_2 and CO mole fractions at different heights as well as ^{14}C isotope measurements, the need for multiple observational datasets limits the time and location for which we have available data. In total, there are seven months (January through July, 2013) that include all of

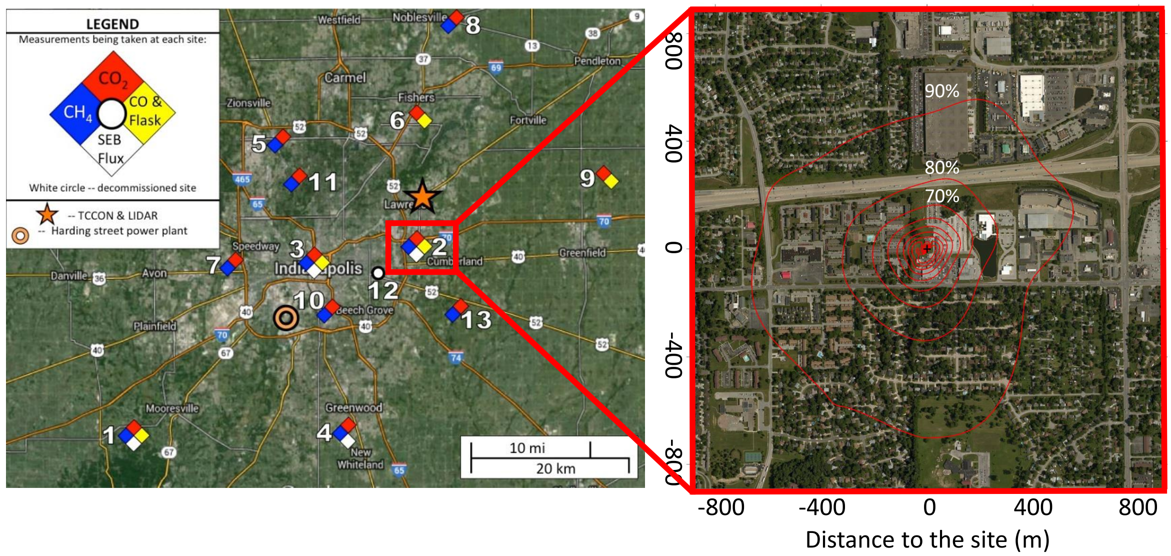

Figure 1: The Indianapolis Flux Experiment (INFLUX) measurement network in Indianapolis, IN (left) and cumulative flux footprints from January to July in 2013 at Tower 2 (right). The contours in the right panel represent the percentage of the time-integrated flux that comes from within that boundary (copyright of the base map belongs to Google Maps). The color of the marker in the left panel represents the measurements at each site: red for CO_2, yellow for CO and ^{14}C, blue for CH_4, and white for surface energy balance fluxes. The coordinates in the right panel are the distance (m) to the measurement site.

these data sets (atmospheric measurements of CO_2 and CO mole fractions, ^{14}C isotope, and CO_2 flux) available at Tower 2 (39.7978°N, 86.0183°W), which is located in a heterogeneous suburban environment (Figures 1 and S1). There is a highway to the north, urban vegetation to the south, and neighborhoods with detached houses. The heterogeneous surroundings present a good test of our ability to partition net CO_2 flux measurements into fossil and biogenic components and to use flux footprint analyses to compare the spatial and temporal heterogeneity of source-specific flux data and the Hestia inventory.

The flux instrumentation, which includes a sonic anemometer (Campbell Scientific, CSAT-3) and a high-frequency open-path infrared CO_2 sensor (LI-COR Environmental, LI-7500), is mounted at 30 m above ground level (AGL) on Tower 2. The eddy-covariance technique measures the covariance between fluctuations in vertical wind velocity and CO_2 density to detect the integrated exchange of CO_2 between land and atmosphere (Lee et al., 2004; Foken and Napo, 2008; Aubinet et al., 2012). We use flux calculation and filtering methods recommended by Vickers and Mahrt (1997). We filter out extreme values outside 3.5 σ range of the data (0.2% of data are filtered out) and nighttime fluxes during weak turbulence conditions when the friction velocity is less than 0.2 m/s (3.6% of data are filtered out) (Gu et al., 2005). Negative fluxes show contributions of photosynthesis to the flux data (Figure S2). Based on the similarity of the diurnal variation of net CO_2 flux measurements (Figure S3), we define the cold season as January to March (JFM) and the warm season as April to July (AMJJ).

2.2. Partitioning Fossil and Biogenic CO_2 Fluxes

To partition fossil and biogenic components from the net CO_2 flux measurements, we apply a flux-gradient method and atmospheric CO measurements. In addition to flux measurements, we also measure CO_2 and CO mole fractions at 10 m and 40 m heights AGL at Tower 2 (Miles et al., 2017). We use the net flux measurement (F_{CO_2}) and vertical gradient in CO_2 mole fraction (∇C_{CO_2}) to solve for the eddy diffusivity (K):

$$K = -\frac{F_{CO_2}}{\nabla C_{CO_2}}, \tag{1}$$

and use that eddy diffusivity and the CO vertical gradient (∇C_{CO}) to solve for the CO flux (F_{CO}):

$$F_{CO} = -K\nabla C_{CO}. \tag{2}$$

The fossil fuel CO_2 emission (F_{CO_2ff}) is estimated by combining the CO flux with the emission ratio (R) of CO to CO_2ff:

$$F_{CO_2ff} = \frac{F_{CO}}{R}, \tag{3}$$

and we attribute the difference between the net flux measurement and the partitioned fossil fuel CO_2 emission to the biogenic CO_2 flux (F_{CO_2bio}):

$$F_{CO_2bio} = F_{CO_2} - F_{CO_2ff}. \tag{4}$$

There are three assumptions in this method: (1) Turbulent eddies are small enough that local scalar gradients are proportional to turbulent fluxes; (2) CO and CO_2 are subject to the same vertical mixing processes; (3) Within the turbulent flux footprint, CO is mainly produced by fossil fuel combustion simultaneously with CO_2ff emissions. We filter out counter-gradient fluxes, and limit the eddy diffusivity and CO flux within 3.5 σ range of their estimates to screen out extreme values caused by tiny denominators. Human respiration, which would appear in this decomposition as a biological flux, is estimated based on the population density of Indianapolis (896 people km^{-2} in the year 2013) multiplied by a typical emission rate of 942 gCO_2 person^{-1} day^{-1} (Prairie and Duarte, 2007).

The emission ratio of CO to CO_2ff is estimated from flask measurements of ^{14}C and CO measurements (Turnbull et al., 2015). The urban CO and ^{14}C enhancements are estimated by the differences between Tower 2 and upwind background sites (Tower 1 or 9 depending on the wind direction). The median and mean values of CO to CO_2ff ratios estimated from these enhancements are 9.52 and 8.98 ppb ppm^{-1} (cold season) and 9.13 and 9.02 ppb ppm^{-1} (warm season) (Figure S4). We use 9 ppb ppm^{-1} as an approximate value to infer CO_2ff emissions. To test the uncertainty of using different ratios on the flux decomposition, we vary the emission ratio to 11 and 7 (9 $\pm$ 2) ppb

ppm^{-1}. These are plausible bounds (Table 2 in Turnbull et al. (2015)) for this flux site, representing approximately the 70^{th} and 30^{th} percentiles of the values. With a linear relation of the flux decomposition to the emission ratio (Equation 3), this maximum and minimum boundary approach represents our limited confidence in the emission ratio and its uncertainty bounds. A more formal error propagation would suggest more confidence than we have in our estimate of the uncertainty in the emission ratio. In addition, since traffic emissions are likely to have a higher ratio and residential emissions have a smaller ratio, we add another scenario with a CO to CO_2ff ratio of 15 ppb ppm^{-1} for northerly winds from the highway and 7 ppb ppm^{-1} for the other wind directions based on sectoral emission ratios estimated by Turnbull et al. (2015).

2.3. Flux Footprint and Emissions Inventory

A flux footprint, which is defined as the contributing area upwind from the measurement site (Leclerc and Foken, 2014), is essential to account for the spatial heterogeneity of emission sources. We use a two-dimensional flux footprint model (https://footprint.kljun.net/) (Kljun et al., 2015, 2004) to match with the Hestia inventory and estimate the emissions predicted by the inventory at the tower location. Flux footprints were computed with a spatial resolution of approximately 2 m. The size of footprint depends on measurement height, surface roughness, and atmospheric thermal stability. The footprint will increase with an increase in measurement height, with a decrease in surface roughness, and with an increase in atmospheric thermal stability (Burba and Anderson, 2010). Tower-based measurements of wind field and boundary layer characteristics are used to estimate the input parameters of the flux footprint model (measurement height above displacement height, roughness length, Obukhov length, friction velocity, mean wind speed, boundary layer height, standard deviation of lateral velocity fluctuations). The displacement height and roughness length are estimated as 6 m and 0.45 m, respectively. The displacement height is estimated to be 0.7 times the local mean building and tree heights (Weng et al., 2013) and the roughness length is computed from the mean wind and momentum fluxes measured at 30 m AGL (Kent et al., 2017; Drew et al., 2013). We estimate the flux footprint (f) for each hourly flux measurement. After interpolating the Hestia inventory to the coordinates of each flux footprint, we weight the hourly Hestia emissions (Q_H) with the spatially-resolved fractional flux contributions (f) at the same time and sum over the domain of flux footprint (R) to produce a spatially-weighted estimate of the Hestia flux that would be measured at the tower (F_H):

$$F_H = \sum_{i=1}^{R} Q_H(x_i, y_i) f(x_i, y_i) \delta x \delta y. \tag{5}$$

The emissions predicted by the Hestia inventory at the tower (F_H) are compared with the partitioned CO_2ff flux measurements (F_{CO_2ff} in Equation 3).

3. Results

Net CO_2 flux measurements, decomposed as a function of time and space, behave as expected given the environment surrounding the tower. Observed CO_2 emissions are larger in the cold season than the warm season (Figure 2a), perhaps due to increased emissions from building heating around the tower (Figures 1 and S1). In the cold season, there are two prominent peaks in emissions likely corresponding to peaks in traffic volume during rush hours. In the warm season, CO_2ff emissions are mixed with photosynthesis and respiration from urban vegetation within the flux footprints. The daytime photosynthetic uptake of CO_2 indicates the role of urban vegetation. The data show high emissions from the north, and lower emissions or net uptake from the south (Figures 2b and 2c), consistent with the highway to the north and urban vegetation to the south of the tower.

Partitioning of the net observed CO_2 fluxes into fossil and biogenic components yields plausible temporal behavior of these flux components (Figure 3). While smaller than the estimated CO_2ff emissions, the magnitude of the cold season daytime (9 to 20 LST) averaged biological uptake is 15% of the mean CO_2ff emissions over the same time period and the ecosystem respiration averaged over nighttime (21 to 8 LST) is 27% of the mean nighttime CO_2ff emissions. These are non-negligible flux magnitudes that need to be considered to obtain accurate CO_2ff emissions (Figure 3a). Human respiration is estimated to be 0.22 μmol m^{-2} s^{-1}, which would contribute about 10% of the average nighttime CO_2bio fluxes in the cold season. A typical pattern of ecosystem fluxes emerges in the warm season (Figure 3b). The warm season CO_2bio fluxes are equal in amplitude to the CO_2ff emissions, emphasizing the importance of accounting for CO_2bio fluxes in attempts to quantify urban CO_2ff emissions. The error bars are the standard errors of the seasonal means, which represent a mixture of day-to-day variability, random measurement errors, and uncertainty in the flux decomposition using a typical emission ratio (9 ppb ppm^{-1}). We will examine the impacts of using different ratios on the flux decomposition.

The seasonally-averaged partitioned CO_2ff emissions estimates show remarkable similarity to the Hestia inventory when matched in space and time using the flux footprint model. Seasonal-mean CO_2ff emissions differ (Hestia minus observed CO_2ff emissions) by 0.36 μmol m^{-2} s^{-1} (3.2% of the mean partitioned CO_2ff emissions) in the cold season (Figure 4a) and 0.62 μmol m^{-2} s^{-1} (9.1% of the mean partitioned CO_2ff emissions) in the warm season (Figure 4b). The corresponding standard deviations (SDs) of the residuals are 8.91 μmol m^{-2} s^{-1} and 7.52 μmol m^{-2} s^{-1}, which include random errors in the flux measurements. The temporal patterns of seasonally-averaged Hestia and the partitioned CO_2ff emissions also agree remarkably well (Figures 4c and 4d). The correlation coefficients of the diurnal variations are 0.86 (cold season) and 0.93 (warm season), and the slopes are 1.13 and 0.95, respectively. The Hestia emissions are smaller during the night and higher during the day compared to the partitioned observations in the cold season (Figures 4c and S5a), and consistently slightly higher

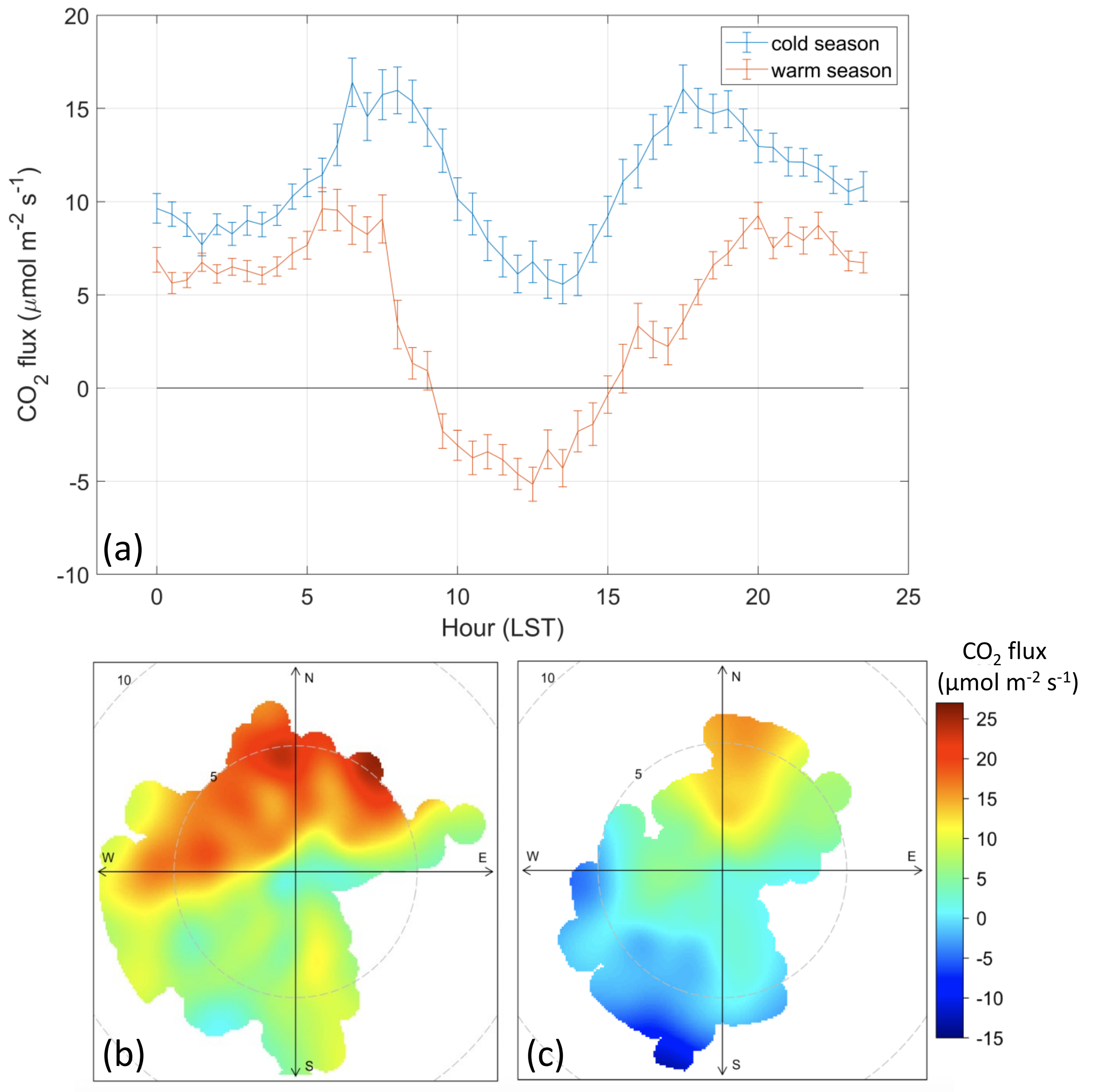

Figure 2: Diurnal variation of seasonally-averaged CO_2 flux measurements during the cold (JFM) and warm (AMJJ) seasons in 2013 (a). Error bars indicate the standard errors of the seasonal means. Spatial variation of time-averaged CO_2 fluxes in the cold (b) and warm (c) seasons. Color indicates flux magnitude. The radial coordinate corresponds to wind speed (m s^{-1}) and the angular coordinate is the wind direction.

than the partitioned observations in the warm season (Figures 4d and S5b).

We also find similarity in the comparison of eddy-covariance and Hestia CO_2ff emissions as a function of wind direction (Figure 5). In the cold season, the Hestia emissions are higher than the observed CO_2ff emissions for all wind directions except the north, west and northwest wind (Table 1). A similar pattern exists in the warm season. Since residential buildings lie upwind in the west and northwest wind directions (Figures 1 and S1), we infer residential emissions could be the source of this discrepancy.

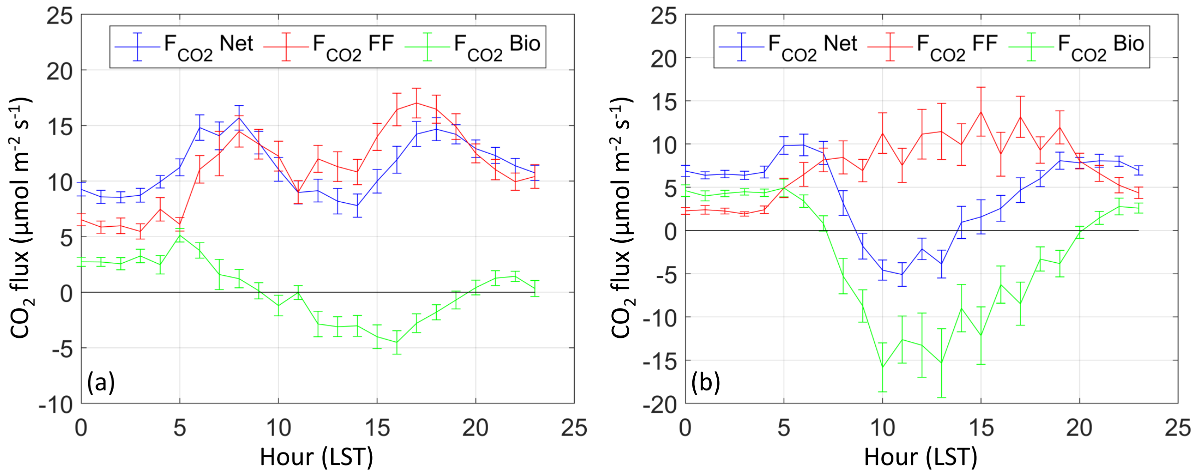

Figure 3: Diurnal variation of seasonally-averaged CO_2 flux measurements (F_{CO2}Net) and the partitioned fossil fuel (F_{CO2}FF) and biogenic (F_{CO2}Bio) fluxes in the cold (JFM) (a) and warm (AMJJ) (b) seasons in 2013. Error bars are the standard errors of the seasonal means.

Table 1: Statistics of flux differences (μmol m^{-2} s^{-1}) between the Hestia inventory and the partitioned fossil fuel CO_2 emissions (Hestia minus observed CO_2ff emissions) for different wind directions.

	DIFF	N	NE	E	SE	S	SW	W	NW
Cold	Median	-2.00	3.32	2.88	3.45	4.14	3.15	-4.47	-2.14
Season	Mean	-1.93	5.88	4.88	3.58	3.84	1.89	-4.72	-1.87
(JFM)	RMSE[a]	10.98	9.27	8.22	5.63	7.45	8.00	10.40	9.06
Warm	Median	2.49	3.34	1.92	1.98	0.98	0.42	-2.71	-4.27
Season	Mean	5.31	3.61	0.92	1.37	0.52	-1.32	-4.17	-5.21
(AMJJ)	RMSE	8.24	9.32	5.19	5.54	5.97	8.62	8.47	13.66

[a]root mean square error

These results are somewhat sensitive to the choice of CO to CO_2ff ratio in the flux decomposition. Seasonal-mean flux bias and bias percentage change significantly when the emission ratio varies from 9 ppb ppm^{-1} to 11 or 7 ppb ppm^{-1} (Figure S6 and Table S1). Figure S6 shows the impact of plausible ratios on the diurnal cycle of the partitioned CO_2ff and CO_2bio fluxes. The lower bound of 7 ppb ppm^{-1} increases the CO_2ff emissions estimate (Figure S6b and Equation 3), thus driving the CO_2bio fluxes down about 3 μmol m^{-2} s^{-1} in the cold season (Figure S6c and Equation 4). This would strengthen the finding of daytime photosynthesis. The upper bound ratio of 11 ppb ppm^{-1} would increase CO_2bio fluxes by about 2 μmol m^{-2} s^{-1} in the cold season, leaving midday fluxes slightly negative and nighttime respiration at about 4 μmol m^{-2} s^{-1}. Similar results are shown in the warm season (Figures S6e and S6f). The magnitude of the partitioned fluxes varies linearly with the change of emission

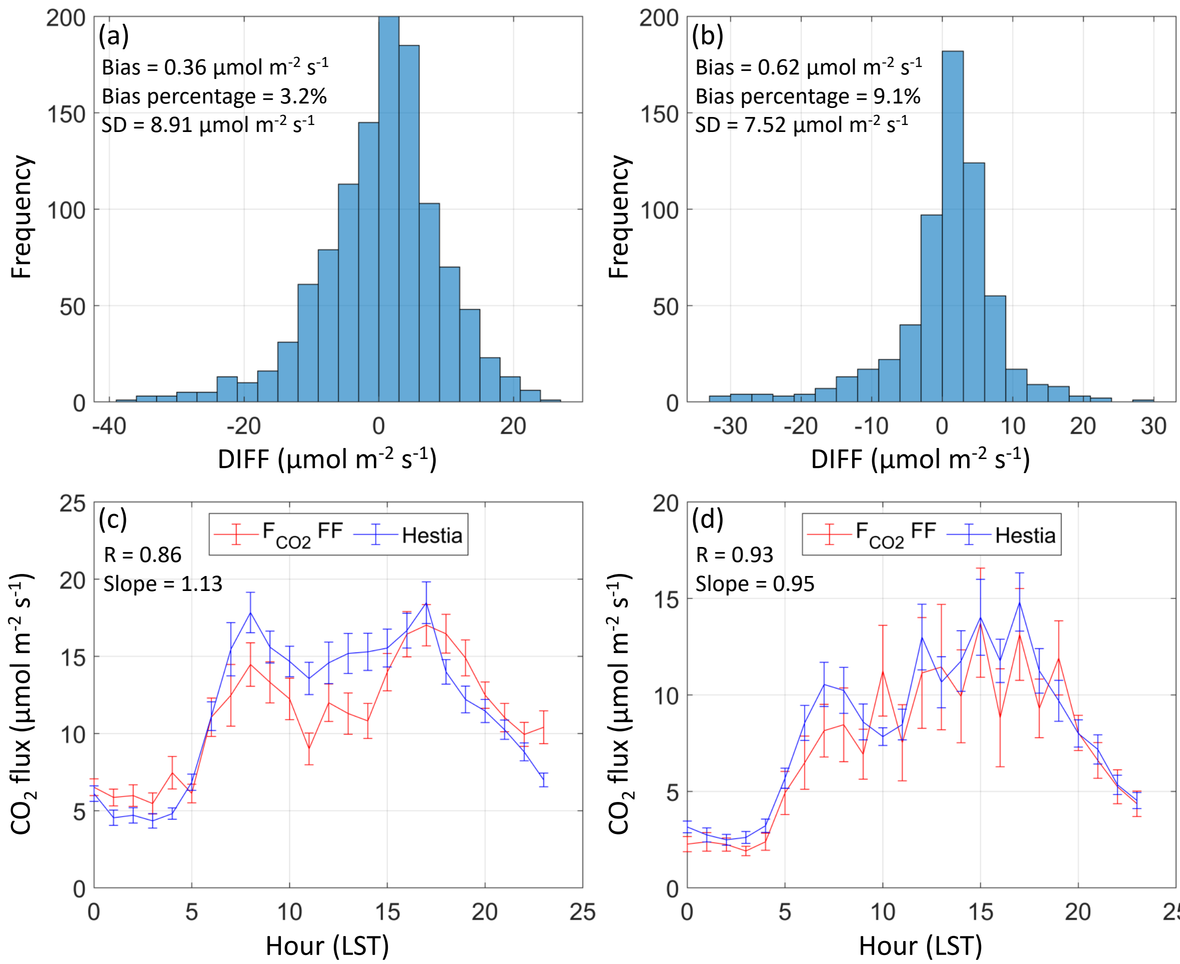

Figure 4: Histogram of flux differences between the Hestia inventory and the partitioned fossil fuel CO_2 emissions (Hestia minus observed CO_2ff emissions) in the cold (JFM) (a) and warm (AMJJ) (b) seasons in 2013. Bias, bias percentage compared to the mean partitioned CO_2ff emissions, and standard deviation (SD) of residuals are listed. Diurnal variation of seasonally-averaged CO_2ff emissions in the cold (c) and warm (d) seasons. Error bars are the standard errors of the seasonal means.

ratio, but the diurnal cycle is not sensitive to this choice. The scenario with the space-varying emission ratio (15 & 7 ppb ppm^{-1}), which may be more realistic than a constant ratio, does not significantly change either the diurnal variation (Figure S6) or the bias estimation (Table S1) when compared to the default scenario (9 ppb ppm^{-1}).

4. Conclusions and Discussion

The remarkable agreement between the Hestia inventory and the partitioned flux measurements suggests that both methods are able to describe the temporal and spatial variability in urban CO_2ff emissions at neighborhood scale. Neither approach has yet been cross-validated at such a high spatial and temporal resolution. The flux

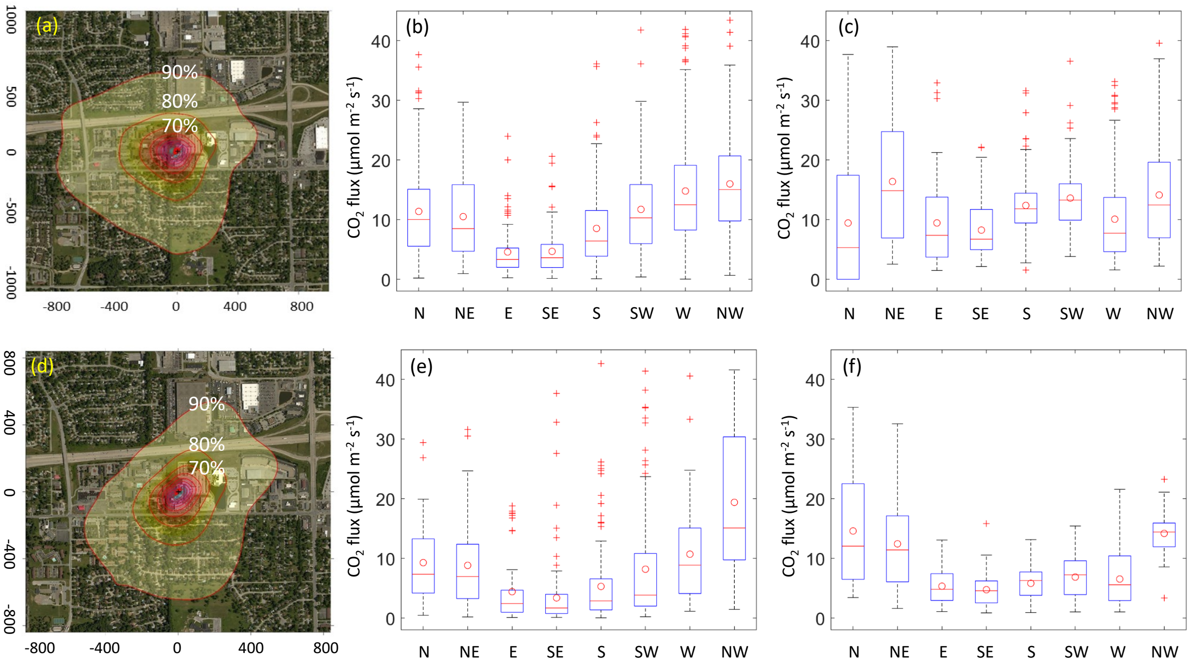

Figure 5: Cumulative flux footprints (a and d), the partitioned fossil fuel CO_2 emissions (b and e) and the Hestia inventory (c and f) for different wind directions. Panels a to c are in the cold season (JFM) and panels d to f are in the warm season (AMJJ) in 2013. The coordinates in the left panel indicate the distance (m) to the measurement site (copyright of the base map belongs to Google Maps). The contours represent the percentage of the time-integrated flux that comes from within that boundary and each contour represents a 10% interval. In the middle and right panels, the red circles, the lines and the plus marks represent the mean, the median and the outliers, respectively. The bottom and top edges of the box indicate the 25th and 75th percentiles. The whiskers extend to the most extreme data points not considered outliers that are defined as more than 1.5 times the interquartile range away from the top or bottom of the box.

measurement partitioning is sensitive to the CO to CO_2ff emission ratio, but the consistency of Hestia and flux data suggests that flask measurements have accurately quantified that ratio. The success of this test suggests that these eddy-covariance flux decomposition methods can be used to quantify source-specific, neighborhood-scale CO_2ff emissions. Further the successful comparison to Hestia suggests that the algorithms and input data used in the inventory system are accurate and precise even at the fine resolution of the eddy-covariance flux measurements.

This study also shows the promise of using this approach for studying urban ecosystem CO_2 fluxes. Previous work has suggested that the edges found in urban ecosystems lead to fundamentally different behavior of these ecosystems (Reinmann et al., 2020). These findings are largely based on chamber-scale flux measurements. It is not clear whether or not, when upscaled to spatial domains that integrate across many edges such as a suburban forest, existing ecosystem models and model parameters will suffice in describing urban CO_2bio fluxes. Current ecosystem models used in urban studies are largely devoid of urban ecosystem flux measurements in either calibration or evaluation due to lack of data (Wu et al., 2021; Hardiman et al., 2017). We suggest that the decomposition methods can serve as a new approach for obtaining ecosystem flux data necessary to develop the next generation of urban ecosystem models.

Finally, this study emphasizes the importance of urban ecosystem fluxes, both in the warm (growing) season and the cold (dormant) season. Our results appear to contradict the findings of Turnbull et al. (2015) who found no net impact of biological CO_2 fluxes on CO_2 enhancements in Indianapolis outside of the growing season. We found the percentage of daytime biological uptake in the cold season is 15% compared to the mean CO_2ff emissions. Our results are consistent with the flask measurements (Figure 5 in Turnbull et al. (2015)) which showed that, for Tower 2, the total CO_2 enhancement in the winter months was 0.8 to 0.9 times the CO_2ff enhancement, suggesting modest net biological uptake of CO_2 during these months within the city. The flask ^{14}C-based CO_2bio enhancement at Tower 2 averaged over the cold season for the three months of this study is -0.37 ppm (Table S2) that is about 10% of the estimated fossil CO_2 enhancement (3.6 ppm), consistent with our eddy-covariance flux measurements. Turnbull et al. (2015) found no net biological CO_2 contribution to the wintertime enhancements when averaging together four towers including Tower 2. The other towers likely have less influence from urban vegetation based on their position around the city. The importance of growing season biological fluxes has been shown in multiple observational (Miller et al., 2020; Turnbull et al., 2015) and inversion (Lauvaux et al., 2020; Sargent et al., 2018; Wu et al., 2018) studies. Uncertainty in biological fluxes has a large impact on inverse flux estimates (Lauvaux et al., 2020; Wu et al., 2018). This flux decomposition approach enables evaluation of the modeled ecosystem flux priors using direct urban ecosystem CO_2 flux measurements. Further, a number of studies (Lauvaux et al., 2016; Heimburger et al., 2017) have made the reasonable assumption of neglecting CO_2bio fluxes in the dormant season. This work shows that urban ecosystems in Indianapolis are moderately active even in the cold season. Additional eddy-covariance flux measurements are needed to study the spatial and temporal variations in urban ecosystem CO_2 fluxes.

Conflict of Interest

The authors declare no competing interests.

Data Availability Statement

The Hestia emission inventory is available at http://dx.doi.org/10.18434/T4/1503341. The eddy-covariance flux measurements and flask data are available on the website (https://sites.psu.edu/influx/data) and the in-situ tower measurements of CO_2 and CO mole fractions are available at http://dx.doi.org/10.18113/D37G6P.

Acknowledgments

The authors thank Bernd J. Haupt (PSU) for data acquisition and quality control. This work was funded by the National Institute of Standards and Technology (Project 70NANB10H245). T. Lauvaux was supported by the French research program Make Our Planet Great Again (Project CIUDAD). K.R. Gurney, J. Liang, and G. Roest received support from the National Aeronautics and Space Administration (Grant NNX14AJ20G) and the National Institute of Standards and Technology (Grant 70NANB16H264N).

References

Ao, X., Grimmond, C., Chang, Y., Liu, D., Tang, Y., Hu, P., Wang, Y., Zou, J. and Tan, J. (2016), Heat, water and carbon exchanges in the tall megacity of Shanghai: challenges and results, *International Journal of Climatology* **36**(14), 4608–4624.

Aubinet, M., Vesala, T. and Papale, D. (2012), *Eddy covariance: a practical guide to measurement and data analysis*, Springer Science & Business Media.

Basu, S., Lehman, S. J., Miller, J. B., Andrews, A. E., Sweeney, C., Gurney, K. R., Xu, X., Southon, J. and Tans, P. P. (2020), Estimating US fossil fuel CO_2 emissions from measurements of ^{14}C in atmospheric CO_2, *Proceedings of the National Academy of Sciences* **117**(24), 13300–13307.

Basu, S., Miller, J. B. and Lehman, S. (2016), Separation of biospheric and fossil fuel fluxes of CO_2 by atmospheric inversion of CO_2 and $^{14}CO_2$ measurements: observation system simulations, *Atmospheric Chemistry and Physics* **16**(9), 5665–5683.

Björkegren, A. and Grimmond, C. (2018), Net carbon dioxide emissions from central London, *Urban Climate* **23**, 131–158.

Boden, T. A., Marland, G. and Andres, R. J. (2009), Global, regional, and national fossil-fuel CO_2 emissions, *Carbon Dioxide Information Analysis Center, Oak Ridge National Laboratory, US Department of Energy, Oak Ridge, Tenn., USA* **10**.

Bréon, F., Broquet, G., Puygrenier, V., Chevallier, F., Xueref-Remy, I., Ramonet, M., Dieudonné, E., Lopez, M., Schmidt, M., Perrussel, O. et al. (2015), An attempt at estimating Paris area CO_2 emissions from atmospheric concentration measurements, *Atmospheric Chemistry and Physics* **15**(4), 1707–1724.

Bulkeley, H. (2013), *Cities and Climate Change*, London: Routledge.

Burba, G. and Anderson, D. (2010), *A brief practical guide to eddy covariance flux measurements: principles and workflow examples for scientific and industrial applications*, Li-Cor Biosciences.

Chaouad, R. and Verzeroli, M. (2018), The urbanization of the world: Facts and challenges, *Revue internationale et strategique* (4), 47–65.

Christen, A. (2014), Atmospheric measurement techniques to quantify greenhouse gas emissions from cities, *Urban Climate* **10**, 241–260.

Christen, A., Coops, N., Crawford, B., Kellett, R., Liss, K., Olchovski, I., Tooke, T., Van Der Laan, M. and Voogt, J. (2011), Validation of modeled carbon-dioxide emissions from an urban neighborhood with direct eddy-covariance measurements, *Atmospheric Environment* **45**(33), 6057–6069.

Davis, K. J., Deng, A., Lauvaux, T., Miles, N. L., Richardson, S. J., Sarmiento, D. P., Gurney, K. R., Hardesty, R. M., Bonin, T. A., Brewer, W. A. et al. (2017), The Indianapolis Flux Experiment (INFLUX): a test-bed for developing urban greenhouse gas emission measurements, *Elem Sci Anth* **5**.

Drew, D. R., Barlow, J. F. and Lane, S. E. (2013), Observations of wind speed profiles over Greater London, UK, using a Doppler lidar, *Journal of Wind Engineering and Industrial Aerodynamics* **121**, 98–105.

Edenhofer, O. et al. (2015), *Climate Change 2014: Mitigation of Climate Change*, Vol. 3, Cambridge University Press.

Foken, T. and Napo, C. J. (2008), *Micrometeorology*, Springer.

Gately, C. and Hutyra, L. (2017), Large uncertainties in urban-scale carbon emissions, *Journal of Geophysical Research: Atmospheres* **122**(20), 11–242.

Grimmond, C., King, T., Cropley, F., Nowak, D. and Souch, C. (2002), Local-scale fluxes of carbon dioxide in urban environments: methodological challenges and results from Chicago, *Environmental Pollution* **116**, S243–S254.

Gu, L., Falge, E. M., Boden, T., Baldocchi, D. D., Black, T., Saleska, S. R., Suni, T., Verma, S. B., Vesala, T., Wofsy, S. C. et al. (2005), Objective threshold determination for nighttime eddy flux filtering, *Agricultural and Forest Meteorology* **128**(3-4), 179–197.

Gurney, K. R., Liang, J., Patarasuk, R., Song, Y., Huang, J. and Roest, G. (2020), The Vulcan version 3.0 high-resolution fossil fuel CO_2 emissions for the United States, *Journal of Geophysical Research: Atmospheres* **125**(19), e2020JD032974.

Gurney, K. R., Mendoza, D. L., Zhou, Y., Fischer, M. L., Miller, C. C., Geethakumar, S. and de la Rue du Can, S. (2009), High resolution fossil fuel combustion CO_2 emission fluxes for the United States, *Environmental Science & Technology* **43**(14), 5535–5541.

Gurney, K. R., Razlivanov, I., Song, Y., Zhou, Y., Benes, B. and Abdul-Massih, M. (2012), Quantification of fossil fuel CO_2 emissions on the building/street scale for a large US City, *Environmental Science & Technology* **46**(21), 12194–12202.

Hardiman, B. S., Wang, J. A., Hutyra, L. R., Gately, C. K., Getson, J. M. and Friedl, M. A. (2017), Accounting for urban biogenic fluxes in regional carbon budgets, *Science of The Total Environment* **592**, 366–372.

Heimburger, A. M., Harvey, R. M., Shepson, P. B., Stirm, B. H., Gore, C., Turnbull, J., Cambaliza, M. O., Salmon, O. E., Kerlo, A.-E. M., Lavoie, T. N. et al. (2017), Assessing the optimized precision of the aircraft mass balance method for measurement of urban greenhouse gas emission rates through averaging, *Elem Sci Anth* **5**.

Helfter, C., Tremper, A. H., Halios, C. H., Kotthaus, S., Bjorkegren, A., Grimmond, C. S. B., Barlow, J. F. and Nemitz, E. (2016), Spatial and temporal variability of urban fluxes of methane, carbon monoxide and carbon dioxide above London, UK, *Atmospheric Chemistry and Physics* **16**(16), 10543–10557.

Hsu, A., Höhne, N., Kuramochi, T., Roelfsema, M., Weinfurter, A., Xie, Y., Lütkehermöller, K., Chan, S., Corfee-Morlot, J., Drost, P. et al. (2019), A research roadmap for quantifying non-state and subnational climate mitigation action, *Nature Climate Change* **9**(1), 11–17.

Hutyra, L. R., Duren, R., Gurney, K. R., Grimm, N., Kort, E. A., Larson, E. and Shrestha, G. (2014), Urbanization and the carbon cycle: Current capabilities and research outlook from the natural sciences perspective, *Earth's Future* **2**(10), 473–495.

Ishidoya, S., Sugawara, H., Terao, Y., Kaneyasu, N., Aoki, N., Tsuboi, K. and Kondo, H. (2020), O_2:CO_2 exchange ratio for net turbulent flux observed in an urban area of Tokyo, Japan, and its application to an evaluation of anthropogenic CO_2 emissions, *Atmospheric Chemistry and Physics* **20**(9), 5293–5308.

Järvi, L., Nordbo, A., Junninen, H., Riikonen, A., Moilanen, J., Nikinmaa, E. and Vesala, T. (2012), Seasonal and annual variation of carbon dioxide surface fluxes in Helsinki, Finland, in 2006–2010, *Atmospheric Chemistry and Physics* **12**(18), 8475–8489.

Kent, C. W., Grimmond, S., Barlow, J., Gatey, D., Kotthaus, S., Lindberg, F. and Halios, C. H. (2017), Evaluation of urban local-scale aerodynamic parameters: implications for the vertical profile of wind speed and for source areas, *Boundary-Layer Meteorology* **164**(2), 183–213.

Kljun, N., Calanca, P., Rotach, M. and Schmid, H. (2004), A simple parameterisation for flux footprint predictions, *Boundary-Layer Meteorology* **112**(3), 503–523.

Kljun, N., Calanca, P., Rotach, M. and Schmid, H. P. (2015), A simple two-dimensional parameterisation for Flux Footprint Prediction (FFP), *Geoscientific Model Development* **8**(11), 3695–3713.

Kunik, L., Mallia, D. V., Gurney, K. R., Mendoza, D. L., Oda, T. and Lin, J. C. (2019), Bayesian inverse estimation of urban CO_2 emissions: results from a synthetic data simulation over Salt Lake City, UT, *Elem Sci Anth* **7**(1).

Lauvaux, T., Gurney, K. R., Miles, N. L., Davis, K. J., Richardson, S. J., Deng, A., Nathan, B. J., Oda, T., Wang, J. A., Hutyra, L. et al. (2020), Policy-relevant assessment of urban CO_2 emissions, *Environmental Science & Technology* **54**(16), 10237–10245.

Lauvaux, T., Miles, N. L., Deng, A., Richardson, S. J., Cambaliza, M. O., Davis, K. J., Gaudet, B., Gurney, K. R., Huang, J., O'Keefe, D. et al. (2016), High-resolution atmospheric inversion of urban CO_2 emissions during the dormant season of the Indianapolis Flux Experiment (INFLUX), *Journal of Geophysical Research: Atmospheres* **121**(10), 5213–5236.

Leclerc, M. Y. and Foken, T. (2014), *Footprints in Micrometeorology and Ecology*, Springer.

Lee, T. and Koski, C. (2014), Mitigating global warming in global cities: comparing participation and climate change policies of C40 cities, *Journal of Comparative Policy Analysis: Research and Practice* **16**(5), 475–492.

Lee, X., Massman, W. and Law, B. (2004), *Handbook of Micrometeorology: A guide for surface flux measurement and analysis*, Springer Science & Business Media.

Levin, I. and Karstens, U. (2007), Inferring high-resolution fossil fuel CO_2 records at continental sites from combined $^{14}CO_2$ and CO observations, *Tellus B* **59**(2), 245–250.

Lietzke, B., Vogt, R., Feigenwinter, C. and Parlow, E. (2015), On the controlling factors for the variability of carbon dioxide flux in a heterogeneous urban environment, *International Journal of Climatology* **35**(13), 3921–3941.

Menzer, O. and McFadden, J. P. (2017), Statistical partitioning of a three-year time series of direct urban net CO_2 flux measurements into biogenic and anthropogenic components, *Atmospheric Environment* **170**, 319–333.

Miles, N. L., Richardson, S. J., Lauvaux, T., Davis, K. J., Balashov, N. V., Deng, A., Turnbull, J. C., Sweeney, C., Gurney, K. R., Patarasuk, R. et al. (2017), Quantification of urban atmospheric boundary layer greenhouse gas dry mole fraction enhancements in the dormant season: results from the Indianapolis Flux Experiment (INFLUX), *Elem Sci Anth* **5**.

Miller, J. B., Lehman, S. J., Montzka, S. A., Sweeney, C., Miller, B. R., Karion, A., Wolak, C., Dlugokencky, E. J., Southon, J., Turnbull, J. C. et al. (2012), Linking emissions of fossil fuel CO_2 and other anthropogenic trace gases using atmospheric $^{14}CO_2$, *Journal of Geophysical Research: Atmospheres* **117**(D8).

Miller, J. B., Lehman, S. J., Verhulst, K. R., Miller, C. E., Duren, R. M., Yadav, V., Newman, S. and Sloop, C. D. (2020), Large and seasonally varying biospheric CO_2 fluxes in the Los Angeles megacity revealed by atmospheric radiocarbon, *Proceedings of the National Academy of Sciences* **117**(43), 26681–26687.

Nemitz, E., Hargreaves, K. J., McDonald, A. G., Dorsey, J. R. and Fowler, D. (2002), Micrometeorological measurements of the urban heat budget and CO_2 emissions on a city scale, *Environmental Science & Technology* **36**(14), 3139–3146.

Oda, T., Bun, R., Kinakh, V., Topylko, P., Halushchak, M., Marland, G., Lauvaux, T., Jonas, M., Maksyutov, S., Nahorski, Z. et al. (2019), Errors and uncertainties in a gridded carbon dioxide emissions inventory, *Mitigation and Adaptation Strategies for Global Change* **24**(6), 1007–1050.

Olivier, J. and Janssens-Maenhout, G. (2012), CO_2 emissions from fuel combustion, *IEA CO_2 report* .

Park, C. and Schade, G. W. (2016), Anthropogenic and biogenic features of long-term measured CO_2 flux in north downtown Houston, Texas, *Journal of Environmental Quality* **45**(1), 253–265.

Prairie, Y. T. and Duarte, C. M. (2007), Direct and indirect metabolic CO_2 release by humanity, *Biogeosciences* **4**(2), 215–217.

Reinmann, A. B., Smith, I. A., Thompson, J. R. and Hutyra, L. R. (2020), Urbanization and fragmentation mediate temperate forest carbon cycle response to climate, *Environmental Research Letters* **15**(11), 114036.

Richardson, S. J., Miles, N. L., Davis, K. J., Lauvaux, T., Martins, D. K., Turnbull, J. C., McKain, K., Sweeney, C. and Cambaliza, M. O. L. (2017), Tower measurement network of in-situ CO_2, CH_4 and CO in support of the Indianapolis Flux (INFLUX) Experiment, *Elem Sci Anth* **5**.

Sargent, M., Barrera, Y., Nehrkorn, T., Hutyra, L. R., Gately, C. K., Jones, T., McKain, K., Sweeney, C., Hegarty, J., Hardiman, B. et al. (2018), Anthropogenic and biogenic CO_2 fluxes in the Boston urban region, *Proceedings of the National Academy of Sciences* **115**(29), 7491–7496.

Silva, S. J., Arellano, A. F. and Worden, H. M. (2013), Toward anthropogenic combustion emission constraints from space-based analysis of urban CO_2/CO sensitivity, *Geophysical Research Letters* **40**(18), 4971–4976.

Staufer, J., Broquet, G., Bréon, F.-M., Puygrenier, V., Chevallier, F., Xueref-Rémy, I., Dieudonné, E., Lopez, M., Schmidt, M., Ramonet, M. et al. (2016), The first 1-year-long estimate of the Paris region fossil fuel CO_2 emissions based on atmospheric inversion, *Atmospheric Chemistry and Physics* **16**(22), 14703–14726.

Stull, R. B. (2012), *An Introduction to Boundary Layer Meteorology*, Springer Science & Business Media.

Sugawara, H., Ishidoya, S., Terao, Y., Takane, Y., Kikegawa, Y. and Nakajima, K. (2021), Anthropogenic CO_2 emissions changes in an urban area of Tokyo, Japan, due to the COVID-19 pandemic: A case study during the state of emergency in April–May 2020, *Geophysical Research Letters* **48**(15), e2021GL092600.

Turnbull, J., Karion, A., Davis, K. J., Lauvaux, T., Miles, N. L., Richardson, S. J., Sweeney, C., McKain, K., Lehman, S. J., Gurney, K. R. et al. (2018), Synthesis of urban CO_2 emission estimates from multiple methods from the Indianapolis Flux Project (INFLUX), *Environmental Science & Technology* **53**(1), 287–295.

Turnbull, J., Karion, A., Fischer, M., Faloona, I., Guilderson, T., Lehman, S., Miller, B., Miller, J., Montzka, S., Sherwood, T. et al. (2011), Assessment of fossil fuel carbon dioxide and other anthropogenic trace gas emissions from airborne measurements over Sacramento, California in spring 2009, *Atmospheric Chemistry and Physics* **11**(2), 705–721.

Turnbull, J., Sweeney, C., Karion, A., Newberger, T., Lehman, S. J., Tans, P. P., Davis, K. J., Lauvaux, T., Miles, N. L., Richardson, S. J. et al. (2015), Toward quantification and source sector identification of fossil fuel CO_2 emissions from an urban area: results from the INFLUX experiment, *Journal of Geophysical Research: Atmospheres* **120**(1), 292–312.

Turner, A. J., Shusterman, A. A., McDonald, B. C., Teige, V., Harley, R. A. and Cohen, R. C. (2016), Network design for quantifying urban CO_2 emissions: assessing trade-offs between precision and network density, *Atmospheric Chemistry and Physics* **16**(21), 13465–13475.

Velasco, E. and Roth, M. (2010), Cities as net sources of CO_2: review of atmospheric CO_2 exchange in urban environments measured by eddy covariance technique, *Geography Compass* **4**(9), 1238–1259.

Vickers, D. and Mahrt, L. (1997), Quality control and flux sampling problems for tower and aircraft data, *Journal of Atmospheric and Oceanic Technology* **14**(3), 512–526.

Vogel, F., Hamme, S., Steinhof, A., Kromer, B. and Levin, I. (2010), Implication of weekly and diurnal ^{14}C calibration on hourly estimates of CO-based fossil fuel CO_2 at a moderately polluted site in southwestern Germany, *Tellus B: Chemical and Physical Meteorology* **62**(5), 512–520.

Vogt, R., Christen, A., Rotach, M., Roth, M. and Satyanarayana, A. (2006), Temporal dynamics of CO_2 fluxes and profiles over a Central European city, *Theoretical and Applied Climatology* **84**(1-3), 117–126.

Weng, Q., Hu, X., Quattrochi, D. A. and Liu, H. (2013), Assessing intra-urban surface energy fluxes using remotely sensed aster imagery and routine meteorological data: A case study in Indianapolis, USA, *IEEE Journal of Selected Topics in Applied Earth Observations and Remote Sensing* **7**(10), 4046–4057.

Wu, D., Lin, J. C., Duarte, H. F., Yadav, V., Parazoo, N. C., Oda, T. and Kort, E. A. (2021), A model for urban biogenic CO_2 fluxes: Solar-Induced Fluorescence for Modeling Urban biogenic Fluxes (SMUrF v1), *Geoscientific Model Development* **14**(6), 3633–3661.

Wu, K., Lauvaux, T., Davis, K. J., Deng, A., Coto, I. L., Gurney, K. R. and Patarasuk, R. (2018), Joint inverse estimation of fossil fuel and biogenic CO_2 fluxes in an urban environment: An observing system simulation experiment to assess the impact of multiple uncertainties, *Elem Sci Anth* **6**(1).